Mechanism of Icariin regulation of the effect of miR-122-5p in osteoblast-derived exosomes on osteogenesis and migration of bone marrow mesenchymal stem cells

Aofei Yang
Hubei Provincial Hospital of Traditional Chinese Medicine
lxz
Wuhan Third Hospital, Tongren Hospital of Wuhan University
Lu Yang
Wuhan Third Hospital, Tongren Hospital of Wuhan University
Haijia Xu
Wuhan Third Hospital, Tongren Hospital of Wuhan University
Jing Hu
Huazhong University of Science & Technology
Hantao Cai
The First People's Hospital of Wenling
Yu Ning
XiangYang Hospital of Traditional Chinese Medicine, Hubei University of Chinese Medicine
Zhanghua Li (lizhanghua_123@163.com)
Wuhan Third Hospital, Tongren Hospital of Wuhan University

Research Article

Keywords: Exosomes, Icariin, miRNA, osteogenic differentiation, migration

Posted Date: June 7th, 2022

DOI: https://doi.org/10.21203/rs.3.rs-280286/v2

Abstract

Background

Avascular necrosis of the femoral head (ANFH) is a common orthopaedic disease due to bone defects. However, few clear methods to treat ANFH in clinical practice are known. Many findings suggest that promoting the osteogenic differentiation and directional migration of stem cells may be a key method for bone regeneration. Over time, an increasing number of researchers have begun to focus on Chinese medicine and Chinese medicinal extracts; Epimedium is the Chinese herbal medicine studied in the most detail in the field of bone regeneration, and Icariin (ICA) is one of the main active ingredients in Epimedium.

Objective

This study aimed to explore the effects of ICA on the osteogenic differentiation and migration of bone marrow mesenchymal stem cells (BMSCs) and reveal its mechanism to provide a theoretical basis for the treatment of ANFH.

Methods

After primary BMSCs were freshly isolated from a normal rabbit and treated with various concentrations of ICA, the activity and proliferation of BMSCs were detected by CCK-8 assay, and the mineralized nodules was detected by Alizarin Red staining, to determine the optimal concentration of ICA. qPCR and western blot were used to demostrate the effects of ICA on the osteogenic differentiation and migration of BMSCs. Osteoblasts-derived exosomes (OB-exos) were extracted and analysed by high-throughput sequencing. Effect of ICA combined with OB-exos were analysed. And miRNA mimic and an miRNA inhibitor were synthetised to verify the osteogenic differentiation and migration of BMSCs alone or co-cultured with ICA.

Results

The CCK-8 assay and Alizarin Red staining showed that the optimal concentration of ICA is 1×10^{-7} M. ICA could effectively promote the osteogenic differentiation and migration of BMSCs, and this could be enhanced after co-culturing with OB-exos. The four miRNAs with the greatest concentrations in the OB-exos were let-7a-5p, miR-100-5p, miR-21-5p and miR-122-5p. qPCR and western blot showed that miR-122-5p mimic has positive effects on the osteogensis and migration, and its inhitiotr has negative effects. Simliarly, they could enhance or inhitor the effects of ICA, which means miR-122-5p may be the target of ICA.

Conclusion

Like the OB-exos, ICA could obviously promote the osteogenic differentiation and migration of BMSCs. The combination of ICA and OB-exos enhanced these effects, in which miR-122-5p plays a pivotal role.

1. Introduction

Avascular necrosis of the femoral head (ANFH) is a common orthopaedic disease in patients between 20 and 50 years of age that mainly manifests as bone defects [1, 2]. Femoral head necrosis and bone mass loss, the basic pathological processes in ANFH, arise when the bone metabolism imbalance that is induced by reduced osteogenic differentiation and active osteoclasts. Because of multi-directional differentiation ability, bone marrow mesenchymal stem cells (BMSCs) and intervention methods to promote osteogenic differentiation and migration have become research hotspots. These methods mainly include drugs, physical stimulation, a weightless environment and so on [3–10]. In recent years, an increasing number of researchers have begun to focus on traditional Chinese medicines and their extracts because of their low toxicity [11].

Epimedium is the Chinese herbal medicine studied in the greatest detail for bone regeneration [12]. Epimedium functions to strengthen muscles and bones, improve the kidneys and produce marrow, as shown by traditional Chinese medicine research [13], and Icariin (ICA, C33H40O15, molecular weight: 676.66) is one of the major active ingredients of Epimedium[14]. ICA can not only promote the proliferation and osteogenic differentiation of BMSCs but also enhance ALP activity and the formation of calcium nodules during osteogenic induction by activating the Wnt/β-catenin pathway [14, 15]. Modern medical research suggests that exosomes are critical for communication between cells because they deliver bioactive components from one cell to another.

Exosomes have been demonstrated to serve as a means of intercellular communication in the body. They can easily transfer bioactive components between cells. Additionally, they may be good drug delivery vectors. Exosomes directly or indirectly regulate the balance of bone metabolism and help to maintain the delicate homeostatic balance in bone [16]. Furthermore, exosomes can promote the osteogenic differentiation of BMSCs, which may be linked to the miRNAs contained within exosomes. Therefore, finding the functional miRNAs of osteoblast-derived exosomes (OB-exos) is critical to understanding the mechanism of exosomes. This study applied ICA and exosomes to treat BMSCs and observed its effect on the directional differentiation of BMSCs. Furthermore, the ability of ICA to promote the osteogenic differentiation and migration of BMSCs was determined. We suggest that ICA regulates a specific miRNA in OB-exos to affect osteogenesis and migration and that the use of ICA and OB-exos have a synergistic effect.

2. Materials And Methods

2.1. Materials and reagents

The following materials and reagents were used: bone marrow mesenchymal stem cell complete medium (MSCM, ScienCell, USA), Osteoblast Medium (OBM, ScienCell, USA), fetal bovine serum (FBS, Gibco, USA), ICA (Sigma-Aldrich, USA), total rna extraction kit (OMEGA Company, USA), rna reverse transcription kit and SYBR Green qPCR kit (TOYOBO, Japan), amd3100 (Invitrogen, USA), lipofectamine 2000 (Invitrogen, USA), CCK-8 kit (Dalian Meilunbio, China), Anti-CD29, anti-CD44, anti-CD45, goat hrp-conjugated anti-rabbit and anti-GAPDH (Abcam, USA), anti-Runx2, anti-Smad5, anti-Smad1, anti-SDF-1α, anti-BMP-2, anti-Tsg101 and anti-Osterix (Bioss, China), anti-Smad8, anti-CXCR4 and anti-CD63 (Santa Cruz, USA), anti-HSP70 (Proteintech, USA), miR-122-5p mimic NC, miR-122-5p mimic, miR-122-5p inhibitor NC and miR-122-5p inhibitor (Guangzhou Ribo Biotechnology Co., Ltd., China).

In our experiments, we used the following equipmental instruments: a carbon dioxide incubator (from Thermo Fisher Scientific, America). Fluorescence inverted microscope (Leica Microsystems, Wetzlar, Germany). The gel imaging system and the Bio-Rad CFX Manager system (Bio-Rad, USA).

2.2. Isolation of primary rabbit BMSCs

Primary BMSCs were isolated using the methods described in our previous study. The extracted cells were resuspended in MSCM and then plated, and the medium was changed at the indicated time. The BMSCs were identified by microscopic observation and flow cytometry [17].

2.3. Isolation of rabbit primary osteoblasts (OBs)

Primary osteoblasts were isolated using the methods described by John [18]. Briefly, the ends and length of the bones of limbs from a 6-month-old new zealand white rabbit were removed, and the periosteum on the bone surface were separated and cut into pieces and centrifuged at 600 ×*g* for 5 min. Then, 0.2% type I collagenase was added, and the mixture was placed in a 37°C thermostat for 3 ~ 4 h. The supernatant was discarded after centrifugation at 600 ×*g* for 5 mins, and the remaining material was washed with PBS containing streptomycin and penicillin. Then, the supernatant was removed after centrifugation at 600 ×*g* for 5 mins, and the centrifugation step was repeated once. Finally, the precipitated cells obtained by removing the supernatant were resuspended in OBM and inoculated in a CO_2 incubator (37°C, 20% O_2, 5% CO_2). The cells were subcultured again when they reached 80%~90% confluence. The cells were observed under a microscope and identified by Giemsa staining and Alizarin red staining.

2.4. Extraction and identification of OB-exos

OBs at passage 3 was cultured and the medium was changed to OBM with exosome depleted fetal bovine serum. The extraction of OB-exos was performed according to the following method:

The supernatant of OBs was centrifuged at 1200 ×*g* for 15 mins to remove cell debris, and the remaining supernatant was transferred into another centrifuge tube that was centrifuged at 4000 ×*g* for 60 mins at 4°C. Then, the supernatant was transferred to an ultracentrifuge tube and centrifuged at 4000 ×*g* for 70 mins at 4°C. The supernatant was discarded, and the ultracentrifugation step was repeated again. The white, flaky precipitate that appeared at the bottom of the centrifuge tube consisted of exosomes. The

supernatant was discarded, and 200 μL of PBS was used to resuspend the exosomes by pipetting to mix, after which the exosomes were stored at -80°C for later use.

2.5. High-throughput sequencing and miRNA analysis of OB-exos

OBs were divided into three independent culture flasks to extract exosomes, and the three obtained exosome samples were assayed by high-throughput sequencing.

2.6. Detection of the effect of ICA on BMSCs osteogenic differentiation and migration

2.6.1. Effects of ICA at different concentrations on the proliferation, osteogenesis and migration of BMSCs

P3 BMSCs were inoculated and the following tests were performed: ICA was diluted to the following concentrations: 1×10^{-9} M, 1×10^{-8} M, 1×10^{-7} M, 1×10^{-6} M, 1×10^{-5} M and 1×10^{-4} M. The activity and proliferation of BMSCs treated with ICA at different concentrations were detected with a CCK-8 assay kit. After 2 weeks of culture, Alizarin Red staining was conducted to observe the formation of mineralized nodules. Total mRNA and protein were extracted from the different groups of BMSCs at 3 and 7 days respectively, and the expression of osteoblast-related and migration-related genes was detected by real-time PCR and Western blot. Through these experiments, we identified the optimal concentration of ICA.

2.6.2. Effect of ICA treatment for different stages on the osteogenic differentiation and migration of BMSCs

P3 BMSCs were inoculated and treated with 1×10^{-7} M ICA or 0 M ICA. The mRNA expression of osteoblast-related and migration-related genes was measured by real-time PCR on days 3, 7 and 14. In addition, the mRNA and protein expression of osteoblast-related and migration-related genes were analysed by real-time PCR and Western blot on days 1, 2, 3, 4, 5, 6, and 7, respectively, .

2.6.3. Effects of ICA on the expression of Runx2 and CXCR4

P3 BMSCs were inoculated and treated with 0 M ICA(blank culture medium), 1×10^{-7} M ICA, 1×10^{-7} M ICA + si-Runx2, or 1×10^{-7} M ICA + AMD3100. The solutions of si-Runx2 were prepared according to the following protocol: a pre-prepared si-Runx2 solution was diluted in DMEM at a ratio of 1:50. The transfection reagent Lipofectamine 2000 was also diluted in DMEM at a ratio of 1:50. The two dilute solutions were incubated at room temperature for 5 minutes, mixed well in equal proportions and incubated for 20 minutes at room temperature. The solution concentration of AMD3100 was 50 μmol/L, and the AMD3100 was added to the corresponding wells. After culture for 3 days, the mRNA expression of osteoblast-related and migration-related genes was detected by real-time PCR.

2.7. Effect of ICA combined with OB-exos on the osteogenic differentiation and migration of BMSCs

The effect of ICA combined with OB-exos on the osteogenic differentiation and migration of BMSCs was carried out as follows: The optimal effective concentration of ICA, 1×10^{-7} M, had been determined in previous experiments, and ICA was used at this concentration for subsequent experiments. P3 BMSCs were divided into blank group, ICA group, OB-exos group, and ICA + OB-exos group. Twenty microlitres of exosomes were contained in the OB-exos group and the ICA + OB-exos group. On the 3rd day, the mRNA and protein expression of genes related to osteogenic differentiation and migration were detected by real-time PCR and Western blot.

2.8. ICA regulated the effect of OB-exos miR-122-5p on the osteogenic differentiation and migration of BMSCs

In the previous experiment, the top twenty most abundant miRNAs in exosomes were screened through high-throughput sequencing, and miR-122-5p was selected for subsequent study. Mimic NC, mimic, inhibitor NC, and inhibitor were purchased from RiboBio. We observed the effect of miR-122-5p and ICA together on the osteogenic differentiation and migration of BMSCs. P3 BMSCs were divided into miR-122-5p mimic NC group, miR-122-5p mimic group, miR-122-5p mimic NC + ICA group, and miR-122-5p mimic + ICA group, miR-122-5p inhibitor NC group, miR-122-5p inhibitor group, miR-122-5p inhibitor NC + ICA group, and miR-122-5p inhibitor + ICA group. The final concentration of the miR-122-5p mimic NC and miR-122-5p mimic was 50 nM, and the final concentration of the miR-122-5p inhibitor NC and miR-122-5p inhibitor was 100 nM. The transfection method was operated according to the instructions. On the 3rd day, the mRNA and protein expression of genes related to osteogenic differentiation and migration were detected by real-time PCR and Western blot.

2.9. Quantitative real-time polymerase chain reaction(qPCR)

Total RNA was extracted using the Total RNA Extraction Kit. RNA was then reverse-transcribed into cDNA by the RNA Reverse Transcription Kit. qRT-PCR was carried out using the SYBR Green PCR Kit. GAPDH was used as endogenous references. All these primers were designed and synthesised by SANGON Biotech Co, Ltd. (Shanghai). The primer sequences used in this study are listed in Table 1. qPCR was performed with a Bio-Rad CFX Manager system.

Table 1
Gene primer sequences

Gene	Primer sequence(5′-3′)
GAPDH	Forward 5-TGGAATCCACTGGCGTCTTC-3
	Reverse 5-GGTTCACGCCCATCACAAAC-3
Runx2	Forward 5-AGCGGTCCACTACGTTACCTG-3
	Reverse 5-TCCGACACGGTCGACCGC-3
BMP-2	Forward 5-GCGAGTTGTATTTCGTAACCA-3
	Reverse 5-GAACGTCCCGATCTCGGAC-3
Osterix	Forward 5-TCCCTGGATATGACTCA TCCCT-3
	Reverse 5-CCAAGGAGTAGGTGTGTTGCC-3
Smad1	Forward 5-CTAGCGTTAGCGACCGAGCGA-3
	Reverse 5-GCAGAGCGGGTTATGCGGA-3
Smad5	Forward 5-GTCGAGGTCAACCTACFCAG-3
	Reverse 5- GACCGGAATATGGCGAGCTC-3
Smad8	Forward 5-CCAGCAAGTGCGTCACCATCC-3
	Reverse 5-GCACTCCAGCGGCTTCAACTC-3
CXCR4	Forward 5-GCAGCAGCAGCTACTTTGACG-3
	Reverse 5-GACTCGTTCAGTTTAACGGGG-3
SDF-1α	Forward 5-ATGCCCCTGCCGATTCTTTG-3
	Reverse 5-GGGCACAGTTTGGAGTGTTGA-3

2.10. Western blot analysis

Total protein was extracted from cells of each group, and the protein concentration was determined using a bicinchoninic acid (BCA) kit. Then, 30 μg total protein was loaded into each lane, separated with polyacrylamide gel electrophoresis (PAGE) at60 V for 30 min and at 120 V for 40 min, and then transferred on to polyvinylidene fluoride (PVDF) membranes. After being blocked with 5% skim milk powder at room temperature for 1 h, the membrane was incubated with following primary antibodies overnight at 4℃, including CD63 (1:500), Hsp70 (1:500), Tsg101 (1:1000, Runx2 (1:500), BMP-2 (1:500), Smad1 (1:1000), Smad5 (1:1000), Smad8 (1:1000), Osterix (1:500), SDF-1 (1:500), CXCR4(1:500) and GAPDH (1:500). After being rinsed three times with TBS containing 0.1% Tween-20, the membrane was incubated with the secondary horseradish peroxidase (HRP)-labeled goat anti-rabbit antibody (1:10000)

for 1 h at room temperature. After being rinsed three times with TBST, the membrane was exposed to a chemiluminescence instrument. The relative expression of protein was measured using the ImagePro Plus 6.0. Three independent experiments were conducted.

2.11. Statistical analysis

SPSS 23.0 statistical software was used to perform statistical analysis. These data are presented by the mean ± SEM. Quantitative data were subjected to the chi-square test. Statistical significance was assessed by Student's t-test or one-way ANOVA followed by Tukey's t-test. A value of $P < 0.05$ was considered to be statistically significant.

3. Results

3.1. Morphological observation and flow cytometry identification of BMSCs

Primary BMSCs were isolated and identified by microscopy and flow cytometry. BMSCs were spindle-shaped and exhibited a swirled shape under different visual fields, as shown in Fig. (1)A. Flow cytometry showed that BMSCs were positive for CD29 and CD44 and negative for CD45 (Fig. (1)B).

3.2. Morphological observation and identification of OBs

Primary OBs that were freshly isolated from the normal rabbit were flat and adopted various shapes (fusiform, polygonal, triangular, etc.,) with protrusions of various lengths with different numbers of nuclei. Additionally, the cytoplasm was abundant, with two nuclei occasionally showing a spiral-like pattern (Fig. (2)A). OBs were fusiform or triangular in shape with a large volume of cytoplasm, as shown by Giemsa staining. The cytoplasm was stained purple-blue, while the nucleus was stained dark blue (Fig. (2)B). A large number of scattered mineralized nodules were observed in the OBs after culture for 2 weeks, and the mineralized nodules were red-orange after Alizarin Red staining (Fig. (2)C).

3.3. Morphology and identification of OB-exos

The culture supernatant of OBs was collected and used to extract OB-exos. The obtained exosomes showed a clear, vesicle-like structure with a particle size between 50 nm ~ 200 nm under different magnifications when different fields of view were examined by transmission electron microscopy (Fig. (3)A). Western blot showed that the exosomes were positive for Tsg101, Hsp70, and CD63 (Fig. (3)B).

3.4. High-throughput sequencing of OB-exos

Exosome were assayed by high-throughput sequencing. We determined the components of the exosomes and the top 20 most abundant miRNAs among all exosomal miRNAs (Fig. (4)A & Fig. (4)B). Among them, the top 20 miRNA target genes were measured with four software programs, and the number of

intersections among the top 4 miRNA target genes are shown in a Venn diagram in Fig. 4C; these miRNA target genes included 200 targets of let-7a-5p, 38 targets of miR-100-5p, 197 targets of miR-21-5p, and 330 targets of miR-122-5p.

3.5. ICA affected the proliferation, osteogenic differentiation and migration of BMSCs

The effects of ICA on the activity, proliferation and mineralization of BMSCs were detected. Compared with that in the control group, 1×10^{-4} M and 1×10^{-5} M ICA had a significant inhibitory effect on cell proliferation when the cells were cultured for 24 hours, while ICA at a concentration of 1×10^{-6} M did not inhibit or promote cell proliferation but promoted cell proliferation at concentrations of 1×10^{-7} M, 1×10^{-8} M, and 1×10^{-9} M. When the cells were cultured for 48 hours, ICA at 1×10^{-4} M, 1×10^{-5} M, and 1×10^{-6} M had a significant inhibitory effect on cell proliferation, but at 1×10^{-9} M, ICA did not inhibit or promote cell proliferation. However, it promoted cell proliferation at concentrations of 1×10^{-7} M and 1×10^{-8} M (Fig. (5)A & Fig. (5)B). After culture for 2 weeks, the Alizarin Red staining results suggested that when the concentration of ICA was 1×10^{-7} M, the mineralized nodules in the cells were the must abundant, and the effect of ICA on mineralization was the greatest (Fig. (5)C).

We also observed the effect of different concentrations of ICA on the osteogenic differentiation and migration of BMSCs. As shown in the figures, on days 3 and 7, co-culture of the BMSCs with ICA at a concentration of 1×10^{-7} M increased the expression of osteogenic-related genes (Runx2, BMP-2, Osterix and Smad1/5/8) and migration-related genes (SDF-1α and CXCR4) ($p < 0.05$), as shown in Fig. (6)A-E.

In addition, we found that ICA impacted the osteogenic differentiation and migration of BMSCs during different stages. Real-time PCR and Western blot showed that the expression of osteogenic-related genes and migration-related genes on the 3rd day, 7th day, and 14th day was higher in the 1×10^{-7} M ICA group than in the 0 M ICA group, and these differences were significant ($p < 0.05$). The mRNA expression of osteogenic-related genes and migration-related genes first peaked on the 3rd day and then peaked a second time on the 7th day, when the expression was highest ($p < 0.05$). In contrast, the expression of osteogenic-related and migration-related proteins first peaked on the 4th day and then peaked a second time on the 7th day, and the difference between the two peaks was statistically significant ($p < 0.05$) (Fig. (7)A ~ D).

To investigate the signalling pathway by which ICA affects the osteogenic differentiation and migration of BMSCs, qPCR was carried out, which indicated a statistically significant difference in the findings from the ICA group, ICA + si-Runx2 group, and ICA + AMD3100 group ($p < 0.05$) (Fig. (8)). These findings illustrated that both si-Runx2 and AMD3100 could effectively inhibit the ability of ICA to promote the osteogenic differentiation and migration of BMSCs.

3.6. ICA combined with OB-exos affected the osteogenic differentiation and migration of BMSCs

P3 BMSCs were divided into four groups and treated with ICA, OB-exos or ICA + OB-exos, normal cells were used as the blank control. Compared with the blank group, the ICA group, OB-exos group and ICA + OB-exos group significantly increased both mRNA and protein expression of osteogenic differentiation-related and migration-related genes, and expression of these genes was higher in the ICA + OB-exos group than in the ICA group or OB-exos group ($p < 0.05$, Fig. (9)A-C). These results indicated that ICA combined with OB-exos significantly promoted BMSCs osteogenic differentiation and migration.

3.7. The effects of ICA on the osteogenic differentiation and migration of BMSCs depends on miR-122-5p in vitro.

How does ICA affect the osteogenic differentiation and migration of BMSCs? As shown in Fig. (10)A-C, compared with NC group, the group treated with ICA and miR-122-5p mimic showed enhanced effects on the osteogenic differentiation and migration of BMSCs. Furthermore, as shown in Fig. (11)A-C, the miR-122-5p inhibitor affected the osteogenic differentiation and migration of the BMSCs. When the miR-122-5p inhibitor was combined with ICA, the expression of osteogenic differentiation- and migration-related factors in the BMSCs decreased, and the difference between groups was statistically significant ($p < 0.05$). The experimental results confirmed that miR-122-5p can significantly affect the osteogenic differentiation and migration of BMSCs, and the effect could be enhanced when combined with ICA.

4. Discussion

Studies have shown that ICA can promote the proliferation and osteogenic differentiation of BMSCs [19–30]. Cao et al. [31] demonstrated that intragastric ICA administration significantly accelerated the formation of calli and fracture healing in rats within 5 months of treatment. Fan et al. found that ICA could promote not only the proliferation of BMSCs in a dose-dependent manner in vitro but also their differentiation into osteoblasts at very low doses of 1×10^{-9} M to 1×10^{-6} M [32]. Interestingly, some researches have suggested that the proliferative and osteogenic effects of ICA could be achieved by inhibiting adipogenic differentiation [33, 35].

Many other studies have shown that the optimal concentration of ICA to improve the osteogenic differentiation of BMSCs is 1×10^{-6} M [32, 34], but most researchers believe that the optimal concentration of ICA improving the osteogenic differentiation of BMSCs is 1×10^{-7} M [19, 20, 35], which has been further confirmed in our study. In our experiments, we also observed that ICA at a high concentration ($> 1\times10^{-5}$ M) had toxic effects on the cells. Most of the cells in the 1×10^{-4} M ICA-treated group died, as shown by the CCK-8 assay, which is consistent with the literature.

In this study, we also found that the mRNA expression of osteogenic differentiation-related and migration-related genes peaked twice after 3 and 7 days, with expression higher on the 7th day. The Western blot results showed that from days 1–7, on the 4th and 7th days, the expression of osteogenic differentiation-related and migration-related proteins peaked twice, with protein expression higher on the 7th day. The

results provide a very important reference for the use of ICA in clinical trials and even its medicinal application. In addition, osteogenic differentiation was positively related to the migration of BMSCs treated with ICA. These results indicate that an optimal window for the treatment of BMSCs with ICA exists and that the treatment effects are periodic, which may be related to cellular metabolism.

The Runx2 signalling axis and CXCR4 signalling axis may maintain cross-talk. Our previous work [36] revealed that there was a connection between osteogenic differentiation and migration mediated by CXCR4, but whether osteogenic differentiation and migration occur together has not been demonstrated. Furthermore, whether osteogenic differentiation initiates migration or migration promotes osteogenic differentiation remains to be determined.

By investigating whether ICA plays a role in the osteogenic differentiation and migration of BMSCs through the Runx2 signalling axis and CXCR4 signalling axis, we found that both si-Runx2 and AMD3100 effectively inhibited the effect of ICA. The results also verified that osteogenic differentiation and migration occur together and are co-regulated; when one is inhibited, the other is also suppressed. Thus, cross-talk between these two signalling axes, which promote and inhibit each other exists.

Exosomes, which have unique structural advantages, could be a good tool for transporting drugs to target cells to exert biological effects [37]. The outer layer of the phospholipid bilayer structure of exosomes can effectively and simultaneously protect the contents from various biological enzymes and maintain the activity of various biological molecules. Studies have reported [38–41] that electroporation, ultrafiltration, centrifugation, co-incubation and other methods can be used to load specific drugs into exosomes through their double-layer lipid structure, which allows the exosomes to carry the specific drug to the target cell, where it takes effect. Based on this special role of exosomes, the potential use of exosomes as pharmaceutical carriers has become an important application.

Our experimental suggested the presence of a concomitant relationship between osteogenic differentiation and migration. The results of qPCR and Western blot showed that OB-exos enhanced the osteogenic differentiation and migration of BMSCs, and the combination of ICA and OB-exos had a greater effect than treatment with ICA or OB-exos alone. These results showed that ICA and OB-exos have a synergistic effect.

How does the simultaneous application of ICA and OB-exos have a synergistic effect? We suggest that the mechanism is essentially based on three factors: Both ICA and OB-exos promoted the osteogenic differentiation and migration of BMSCs, but the effects were not simply additive. ICA efficiently entered BMSCs through the transport function of OB-exos to exert its biological effects, and the OB-exos also simultaneously exerted biological effects on the BMSCs. ICA acted not only through the transport function of OB-exos but also by regulating and enhancing the expression of miRNAs in OB-exos. The hypotheses above need to be verified.

Because the composition of OB-exos is very complicated, we expected to find the target miRNA through comprehensive analysis of OB-exos. High-throughput sequencing allows researchers to obtain more

accurate sequencing informatio. In our experiments, we found that miRNAs accounted for 17.47% of the total exosomal content, which indicated the presence of abundant miRNAs in the OB-exos, and the levels of individual mRNAs were also clearly different. A higher miRNA content indicates a closer relationship with osteogenic differentiation. However, some miRNAs may be extremely abundant in different exosomes, and further analysis is needed.

In the next experiment, we selected the top 20 most abundant miRNAs. First, we searched for target genes related to the regulation of bone metabolism in a predicted target gene library through software prediction to screen out miRNAs related to osteogenic differentiation. We identified miR-let-7a-5p, miR-100-5p, and miR-21-5p, none of which were “bone”-related genes in the top 3 gene banks, and a qualified gene in the candidate gene library for miR-122-5p, miR-122-5p, was ranked 4th. Our previous study have showed that miR-122-5p can clearly promote the proliferation of osteoblasts [42]. MiR-122-5p has been explored in many diseases, including acute kidney injury [43], cardiomyocyte injury [44], gastric cancer [45–48], kidney cancer [49], non-alcoholic steatohepatitis [50], breast cancer [51], and cervical cancer [52]. However, little information related to the regulation of osteogenic differentiation and migration in BMSCs.

In our study, the mRNA and protein expression of osteogenic differentiation-related and migration-related genes was found to be obviously increased when miR-122-5p mimic and miR-122-5p mimic + ICA were applied, while miR-122-5p inhibitor and miR-122-5p inhibitor + ICA significantly inhibited their expression. These results suggest that miR-122-5p may work by activating the interrelated genes of the Runx2 signalling axis and CXCR4 signalling axis. At the same time, the expression of these genes was greater in the presence of ICA. In summary, these results demonstrate that miR-122-5p plays a pivotal role in the effect of ICA.

We suggest that miR-122-5p is a target miRNA that regulates the differentiation and migration of BMSCs. The mechanism may be as follows: ICA promotes the osteogenic differentiation and migration of BMSCs through miR-122-5p; miR-122-5p is an effect medium of OB-exos. However, understanding how ICA and miR-122-5p target genes related to the Runx2 and CXCR4 signalling axes for activation requires further study.

5. Conclusion

Both ICA and OB-exos alone could effectively promote the osteogenic differentiation and migration of BMSCs. And the combination of ICA and OB-exos enhanced their effects. Furthermore, miR-122-5p maybe a target miRNA involved in this process.

Declarations

ETHICS APPROVAL AND CONSENT TO PARTICIPATE

All animal experiments were approved by the Ethics Committee of Wuhan Third Hospital(grant no. SY2019-025), Tongren Hospital of Wuhan University and followed the Guide for the Care and Use of

Laboratory Animals. All animal experiments were conducted in the Animal Management Center of Wuhan Third Hospital, Tongren Hospital of Wuhan University. All efforts were made to minimize the number and suffering of the included animals.

HUMAN AND ANIMAL RIGHTS

No humans were used. All animal experiments were conducted in the Animal Management Center of Wuhan Third Hospital, Tongren Hospital of Wuhan University, in accordance with the Guide for the Care and Use of Laboratory Animals.

CONSENT FOR PUBLICATION

Not applicable.

AVAILABILITY OF DATA AND MATERIALS

Not applicable.

FUNDING

This work was supported by Natural Science Foundation of Hubei Province (grant no. zrms2020001525); Hubei Province Traditional Chinese Medicine Research Project (Young Talent Project) (grant no. ZY2021Q014); Health Commission of Hubei Province scientific research project (grant no. WJ2021M010); the Health Family Planning Research Fund of Wuhan City (grant no. WX18M01, WX20D91); the Wuhan Application Foundation Frontier Project (grant no. 2019020701011471); Wuhan Young and Middle-aged Medical Personnel Training Project (grant no. 201987). Project of science and Technology Bureau of Xiangyang City (2020YL25).

CONFLICT OF INTEREST

The authors declare no conflict of interest, financial or otherwise.

ACKNOWLEDGEMENTS

Declared None.

References

1. Wang W, Li Y, Guo Y, et al. Initial displacement as a risk factor for avascular necrosis of the femoral head in pediatric femoral neck fractures: a review of one hundred eight cases. Int Orthop 2020; 44(1):129-139. https://doi.org/10.1007/s00264-019-04429-4 PMID: 31655884
2. Xu YX, Ren YZ, Zhao ZP, et al. Hip survival rate in the patients with avascular necrosis of femoral head after transtrochanteric rotational osteotomy: a systematic review and meta-analysis. Chin Med

J (Engl) 2019; 132(24):2960-2971. https://doi.org/10.1097/CM9.0000000000000562 PMID: 31855958

3. Ye J, Wei D, Peng L, et al. Ginsenoside Rb1 prevents steroid-induced avascular necrosis of the femoral head through the bone morphogenetic protein-2 and vascular endothelial growth factor pathway. Mol Med Rep 2019; 20(4):3175-3181. https://doi.org/10.3892/mmr.2019.10553 PMID: 31432121
4. Huang XZ, Huang J, Li WZ, et al. LncRNA-MALAT1 promotes osteogenic differentiation through regulating ATF4 by sponging miR-214: Implication of steroid-induced avascular necrosis of the femoral head. Steroids 2020; 154:108533. https://doi.org/10.1016/j.steroids.2019.108533 PMID: 31678133
5. Wu T, Shu T, Kang L, et al. Icaritin, a novel plant-derived osteoinductive agent, enhances the osteogenic differentiation of human bone marrow- and human adipose tissue-derived mesenchymal stem cells. Int J Mol Med 2017; 39(4):984-992. https://doi.org/10.3892/ijmm.2017.2906 PMID: 28260001
6. Yan Z, Guo Y, Wang Y, et al. MicroRNA profiles of BMSCs induced into osteoblasts with osteoinductive medium. Exp Ther Med 2018; 15(3):2589-2596. https://doi.org/10.3892/etm.2018.5723 PMID: 29456662
7. Sanghani-Kerai A, McCreary D, Lancashire H, et al. Stem Cell Interventions for Bone Healing: Fractures and Osteoporosis. Curr Stem Cell Res Ther 2018; 13(5):369-377. https://doi.org/10.2174/1574888X13666180410160511 PMID: 29637866
8. Heydari Asl S, Hosseinpoor H, Parivar K, et al. Physical stimulation and scaffold composition efficiently support osteogenic differentiation of mesenchymal stem cells. Tissue Cell 2018; 50:1-7. https://doi.org/10.1016/j.tice.2017.11.001 PMID: 29429509
9. Song F, Jiang D, Wang T, et al. Mechanical Stress Regulates Osteogenesis and Adipogenesis of Rat Mesenchymal Stem Cells through PI3K/Akt/GSK-3β/β-Catenin Signaling Pathway. Biomed Res Int 2017; 2017:6027402. https://doi.org/10.1155/2017/6027402 PMID: 28286769
10. Jin YZ, Lee JH. Mesenchymal Stem Cell Therapy for Bone Regeneration. Clin Orthop Surg 2018; 10(3):271-278. https://doi.org/10.4055/cios.2018.10.3.271 PMID: 30174801
11. Lin AX, Chan G, Hu Y, et al. Internationalization of traditional Chinese medicine: current international market, internationalization challenges and prospective suggestions. Chin Med 2018; 13:9. https://doi.org/10.1186/s13020-018-0167-z PMID: 29449877
12. Wang Z, Wang D, Yang D, et al. The effect of icariin on bone metabolism and its potential clinical application. Osteoporos Int 2018; 29(3):535-544. https://doi.org/10.1007/s00198-017-4255-1 PMID: 29110063
13. Liu Y, Zuo H, Liu X, et al. The antiosteoporosis effect of icariin in ovariectomized rats: a systematic review and meta-analysis. Cell Mol Biol (Noisy-le-grand) 2017; 63(11):124-131. https://doi.org/10.14715/cmb/2017.63.11.22 PMID: 29208188

14. Yang A, Yu C, Lu Q, et al. Mechanism of Action of Icariin in Bone Marrow Mesenchymal Stem Cells. Stem Cells Int 2019; 2019:5747298. https://doi.org/10.1155/2019/5747298 PMID: 31089330
15. Gao J, Xiang S, Wei X, et al. Icariin Promotes the Osteogenesis of Bone Marrow Mesenchymal Stem Cells through Regulating Sclerostin and Activating the Wnt/β-Catenin Signaling Pathway. Biomed Res Int 2021; 2021:6666836. https://doi.org/10.1155/2021/6666836 PMID: 33553429
16. Qin Y, Sun R, Wu C, et al. Exosome: A Novel Approach to Stimulate Bone Regeneration through Regulation of Osteogenesis and Angiogenesis. Int J Mol Sci 2016; 17(5):712. https://doi.org/10.3390/ijms17050712 PMID: 27213355
17. Xu HJ, Liao W, Liu XZ, et al. Down-regulation of exosomal microRNA-224-3p derived from bone marrow-derived mesenchymal stem cells potentiates angiogenesis in traumatic osteonecrosis of the femoral head. FASEB J 2019; 33(7):8055-8068. https://doi.org/10.1096/fj.201801618RRR PMID: 30964699
18. Yee JA. Properties of osteoblast-like cells isolated from the cortical endosteal bone surface of adult rabbits. Calcif Tissue Int 1983; 35(4-5):571-577. https://doi.org/10.1007/BF02405096 PMID: 6311381
19. Wei Q, Zhang J, Hong G, et al. Icariin promotes osteogenic differentiation of rat bone marrow stromal cells by activating the ERα-Wnt/β-catenin signaling pathway. Biomed Pharmacother 2016; 84:931-939. https://doi.org/10.1016/j.biopha.2016.09.107 PMID: 27764755
20. Wei Q, He M, Chen M, et al. Icariin stimulates osteogenic differentiation of rat bone marrow stromal stem cells by increasing TAZ expression. Biomed Pharmacother 2017; 91:581-589. https://doi.org/10.1016/j.biopha.2017.04.019 PMID: 28486190
21. Shi W, Gao Y, Wang Y, et al. The flavonol glycoside icariin promotes bone formation in growing rats by activating the cAMP signaling pathway in primary cilia of osteoblasts. J Biol Chem 2017; 292(51):20883-20896. https://doi.org/10.1074/jbc.M117.809517 PMID: 29089388
22. Zhang ZB, Yang QT. The testosterone mimetic properties of icariin. Asian J Androl 2006; 8(5):601-605. https://doi.org/10.1111/j.1745-7262.2006.00197.x PMID: 16751992
23. Jiao F, Tang W, Huang H, et al. Icariin Promotes the Migration of BMSCs In Vitro and In Vivo via the MAPK Signaling Pathway. Stem Cells Int 2018; 2018:2562105. https://doi.org/10.1155/2018/2562105 PMID: 30319696
24. Zhang X, Han N, Li G, et al. Local icariin application enhanced periodontal tissue regeneration and relieved local inflammation in a minipig model of periodontitis. Int J Oral Sci 2018; 10(2):19. https://doi.org/10.1038/s41368-018-0020-3 PMID: 29895944
25. Fu X, Li S, Zhou S, et al. Stimulatory effect of icariin on the proliferation of neural stem cells from rat hippocampus. BMC Complement Altern Med 2018; 18(1):34. https://doi.org/10.1186/s12906-018-2095-y PMID: 29378551
26. Le AW, Wang ZH, Dai XY, et al. An experimental study on the use of icariin for improving thickness of thin endometrium. Genet Mol Res 2017; 16(1):10.4238/gmr16019126. https://doi.org/10.4238/gmr16019126 PMID: 28128406

27. Xu HB, Huang ZQ. Icariin enhances endothelial nitric-oxide synthase expression on human endothelial cells in vitro. Vascul Pharmacol 2007; 47(1):18-24. https://doi.org/10.1016/j.vph.2007.03.002 PMID: 17499557
28. Liu D, Ye Y, Xu L, et al. Icariin and mesenchymal stem cells synergistically promote angiogenesis and neurogenesis after cerebral ischemia via PI3K and ERK1/2 pathways. Biomed Pharmacother 2018; 108:663-669. https://doi.org/10.1016/j.biopha.2018.09.071 PMID: 30245466
29. Liu T, Zhang X, Luo Y, et al. Slowly Delivered Icariin/Allogeneic Bone Marrow-Derived Mesenchymal Stem Cells to Promote the Healing of Calvarial Critical-Size Bone Defects. Stem Cells Int 2016; 2016:1416047. https://doi.org/10.1155/2016/1416047 PMID: 27721833
30. Chen B, Niu SP, Wang ZY, et al. Local administration of icariin contributes to peripheral nerve regeneration and functional recovery. Neural Regen Res 2015; 10(1):84-89. https://doi.org/10.4103/1673-5374.150711 PMID: 25788925
31. Cao H, Zhang Y, Qian W, et al. Effect of icariin on fracture healing in an ovariectomized rat model of osteoporosis. Exp Ther Med 2017; 13(5):2399-2404. https://doi.org/10.3892/etm.2017.4233 PMID: 28565854
32. Fan JJ, Cao LG, Wu T, et al. The dose-effect of icariin on the proliferation and osteogenic differentiation of human bone mesenchymal stem cells. Molecules 2011; 16(12):10123-10133. https://doi.org/10.3390/molecules161210123 PMID: 22146373
33. Zhang S, Feng P, Mo G, et al. Icariin influences adipogenic differentiation of stem cells affected by osteoblast-osteoclast co-culture and clinical research adipogenic. Biomed Pharmacother 2017; 88:436-442. https://doi.org/10.1016/j.biopha.2017.01.050 PMID: 28122309
34. Huang Z, Cheng C, Cao B, et al. Icariin Protects against Glucocorticoid-Induced Osteonecrosis of the Femoral Head in Rats. Cell Physiol Biochem 2018; 47(2):694-706. https://doi.org/10.1159/000490023 PMID: 29794448
35. Ye Y, Jing X, Li N, et al. Icariin promotes proliferation and osteogenic differentiation of rat adipose-derived stem cells by activating the RhoA-TAZ signaling pathway. Biomed Pharmacother 2017; 88:384-394. https://doi.org/10.1016/j.biopha.2017.01.075 PMID: 28122303
36. Li Z, Wang W, Xu H, et al. Effects of altered CXCL12/CXCR4 axis on BMP2/Smad/Runx2/Osterix axis and osteogenic gene expressions during osteogenic differentiation of MSCs. Am J Transl Res 2017; 9(4):1680-1693. PMID: 28469774
37. Gilligan KE, Dwyer RM. Engineering Exosomes for Cancer Therapy. Int J Mol Sci 2017; 18(6):1122. https://doi.org/10.3390/ijms18061122 PMID: 28538671
38. Emam SE, Ando H, Lila ASA, et al. Liposome co-incubation with cancer cells secreted exosomes (extracellular vesicles) with different proteins expressions and different uptake pathways. Sci Rep 2018; 8(1):14493. https://doi.org/10.1038/s41598-018-32861-w PMID: 30262875
39. Yuana Y, Jiang L, Lammertink BHA, et al. Microbubbles-Assisted Ultrasound Triggers the Release of Extracellular Vesicles. Int J Mol Sci 2017; 18(8):1610. https://doi.org/10.3390/ijms18081610 PMID: 28757579

40. Wang J, Yao Y, Wu J, et al. Identification and analysis of exosomes secreted from macrophages extracted by different methods. Int J Clin Exp Pathol 2015; 8(6):6135-6142. PMID: 26261491
41. Akers JC, Ramakrishnan V, Yang I, et al. Optimizing preservation of extracellular vesicular miRNAs derived from clinical cerebrospinal fluid. Cancer Biomark 2016; 17(2):125-132. https://doi.org/10.3233/CBM-160609 PMID: 27062568
42. Liao W, Ning Y, Xu HJ, et al. BMSC-derived exosomes carrying microRNA-122-5p promote proliferation of osteoblasts in osteonecrosis of the femoral head. Clin Sci (Lond) 2019; 133(18):1955-1975. https://doi.org/10.1042/CS20181064 PMID: 31387936
43. Cheng Q, Wang L. LncRNA XIST serves as a ceRNA to regulate the expression of ASF1A, BRWD1M, and PFKFB2 in kidney transplant acute kidney injury via sponging hsa-miR-212-3p and hsa-miR-122-5p. Cell Cycle 2020; 19(3):290-299. https://doi.org/10.1080/15384101.2019.1707454 PMID: 31914881
44. Peng H, Luo Y, Ying Y. lncRNA XIST attenuates hypoxia-induced H9c2 cardiomyocyte injury by targeting the miR-122-5p/FOXP2 axis. Mol Cell Probes 2020; 50:101500. https://doi.org/10.1016/j.mcp.2019.101500 PMID: 31887421
45. Maruyama S, Furuya S, Shiraishi K, et al. miR-122-5p as a novel biomarker for alpha-fetoprotein-producing gastric cancer. World J Gastrointest Oncol 2018; 10(10):344-350. https://doi.org/10.4251/wjgo.v10.i10.344 PMID: 30364858
46. Zhu XL, Ren LF, Wang HP, et al. Plasma microRNAs as potential new biomarkers for early detection of early gastric cancer. World J Gastroenterol 2019; 25(13):1580-1591. https://doi.org/10.3748/wjg.v25.i13.1580 PMID: 30983818
47. Meng L, Chen Z, Jiang Z, et al. MiR-122-5p suppresses the proliferation, migration, and invasion of gastric cancer cells by targeting LYN. Acta Biochim Biophys Sin (Shanghai) 2020; 52(1):49-57. https://doi.org/10.1093/abbs/gmz141 PMID: 31828293
48. Zhang Y, Huang H, Zhang Y, et al. Combined Detection of Serum MiR-221-3p and MiR-122-5p Expression in Diagnosis and Prognosis of Gastric Cancer. J Gastric Cancer 2019; 19(3):315-328. https://doi.org/10.5230/jgc.2019.19.e28 PMID: 31598374
49. Wang S, Zheng W, Ji A, et al. Overexpressed miR-122-5p Promotes Cell Viability, Proliferation, Migration And Glycolysis Of Renal Cancer By Negatively Regulating PKM2. Cancer Manag Res 2019; 11:9701-9713. https://doi.org/10.2147/CMAR.S225742 PMID: 31814765
50. Zhao Z, Zhong L, Li P, et al. Cholesterol impairs hepatocyte lysosomal function causing M1 polarization of macrophages via exosomal miR-122-5p. Exp Cell Res 2020; 387(1):111738. https://doi.org/10.1016/j.yexcr.2019.111738 PMID: 31759057
51. Zhang W, Jiang H, Chen Y, et al. Resveratrol chemosensitizes adriamycin-resistant breast cancer cells by modulating miR-122-5p. J Cell Biochem 2019; 120(9):16283-16292. https://doi.org/10.1002/jcb.28910 PMID: 31155753
52. Li Y, Wang H, Huang H. Long non-coding RNA MIR205HG function as a ceRNA to accelerate tumor growth and progression via sponging miR-122-5p in cervical cancer. Biochem Biophys Res Commun

2019; 514(1):78-85. https://doi.org/10.1016/j.bbrc.2019.04.102 PMID: 31023531

Figures

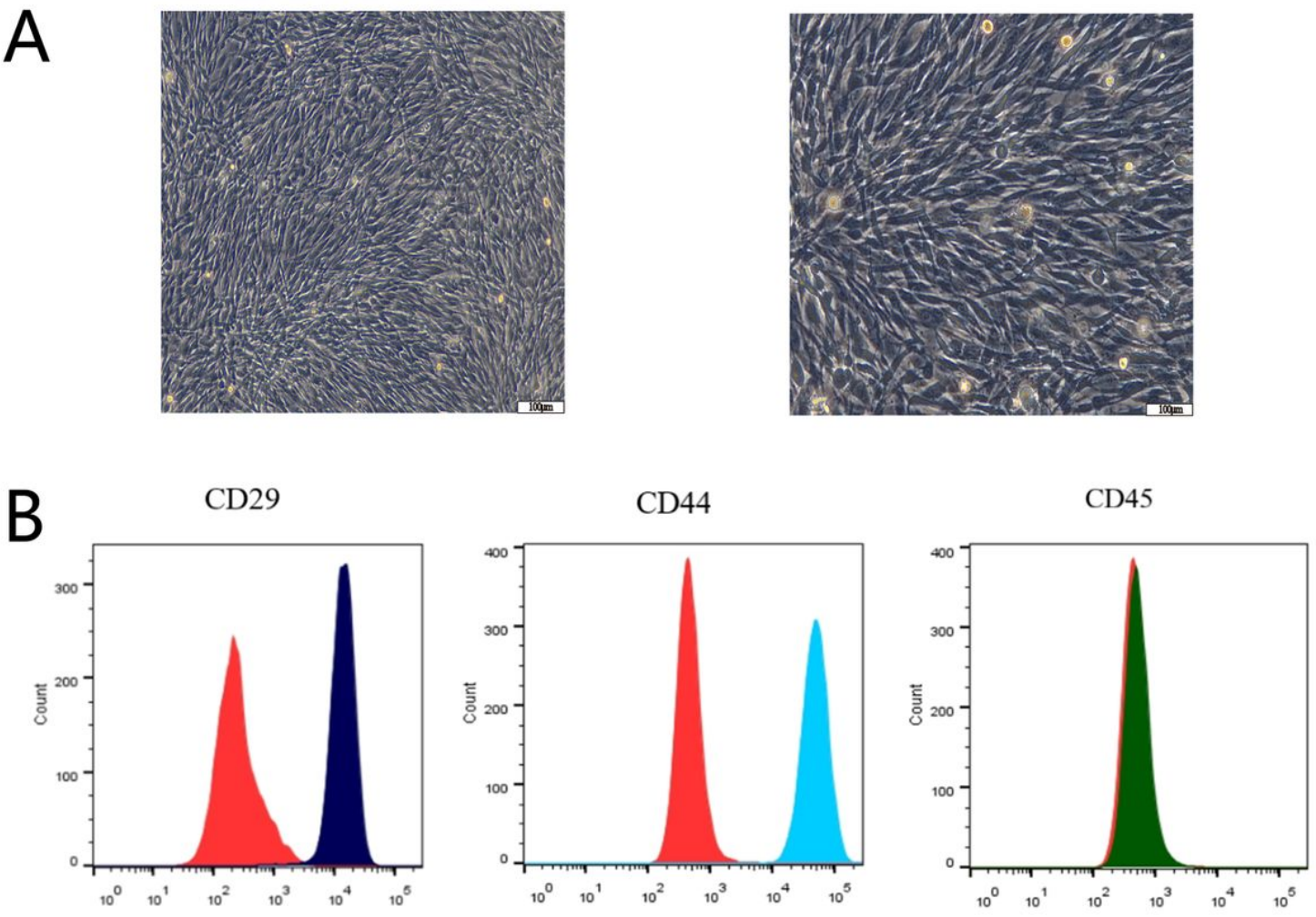

Figure 1

Cultivation and identification of BMSCs. (A) The morphology of P3 BMSCs was observed by microscopy at different magnifications. (B) Flow cytometry was used to identify cell surface markers (CD29, CD44, CD45).

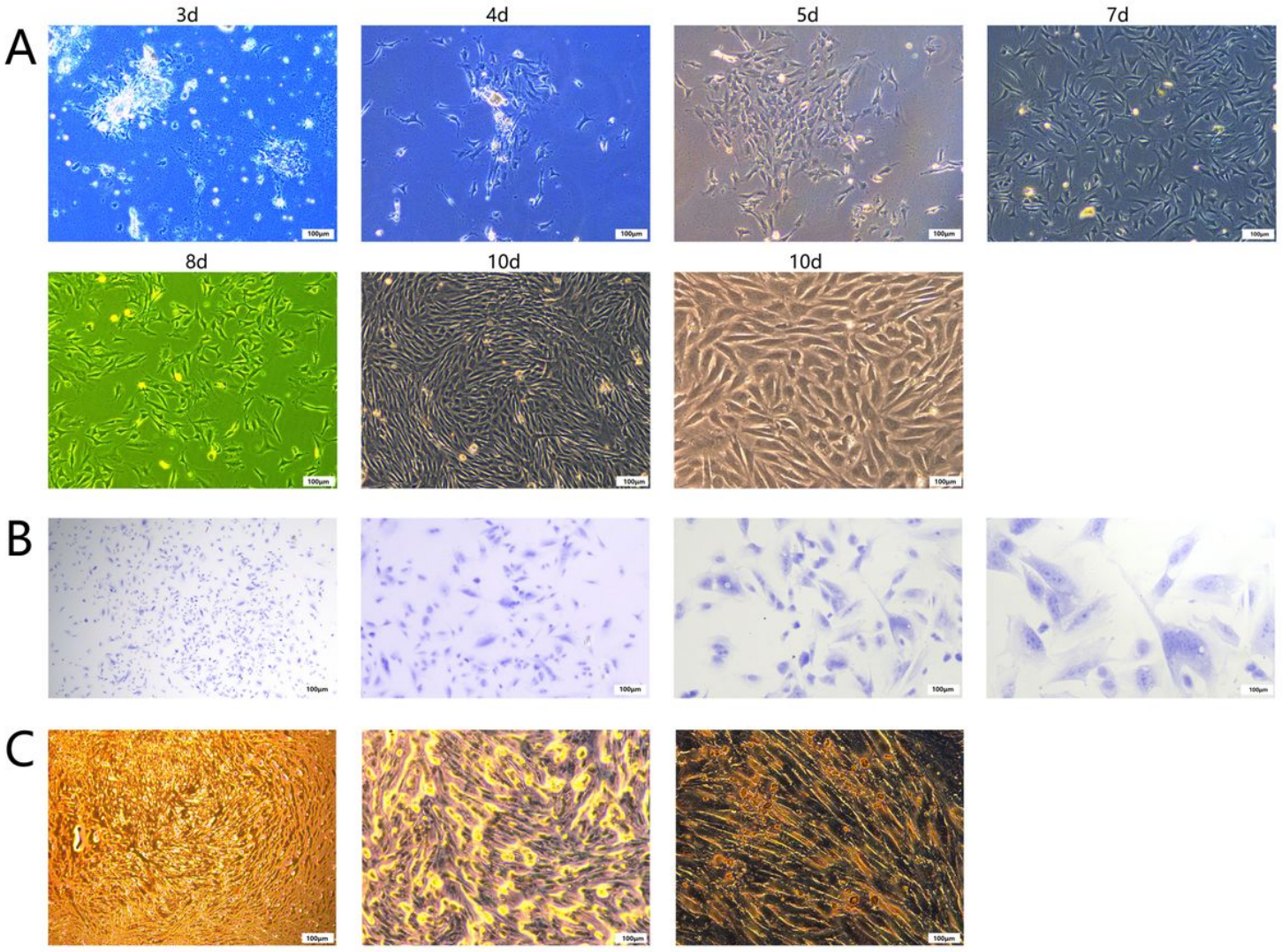

Figure 2

Cultivation and identification of OBs. (A) OBs were examined by microscopy. Primary OBs were extracted and cultured, and we recorded the condition of the cells after their culture on the 3rd day to the 10th day. Cells migrated slowly and continued to proliferate rapidly. (B) OBs were observed by microscopy at different magnifications though Giemsa staining. (C) The mineralized nodules of OBs were screened by alizarin red staining and observed by microscopy at different magnifications after culture for 2 weeks.

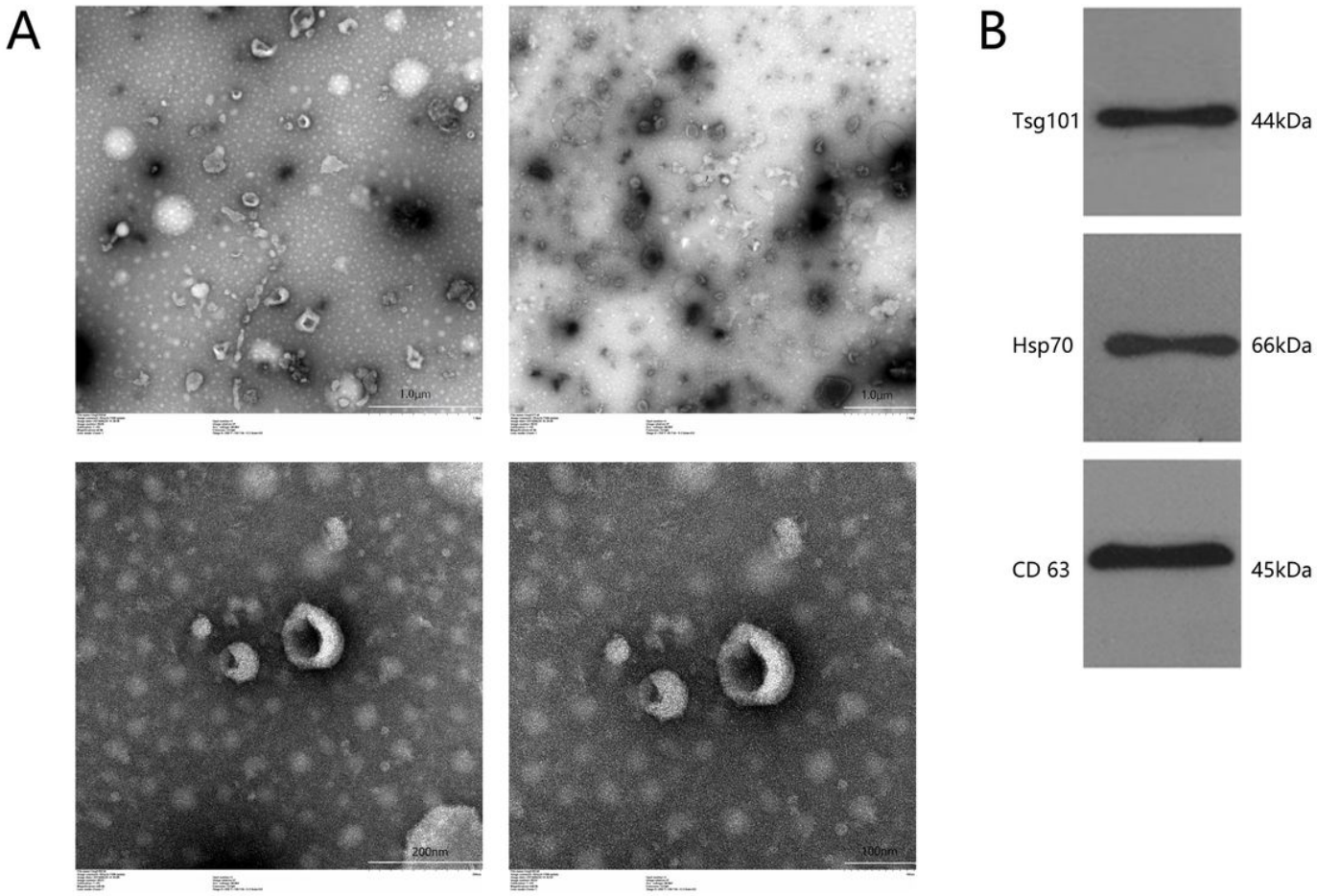

Figure 3

Extraction and identification of OB-exos. (A) Exosomes were identified by transmission electron microscopy in different fields. (B) Western blot was used to identify marker proteins for exosomes: Tsg101, Hsp70, and CD63.

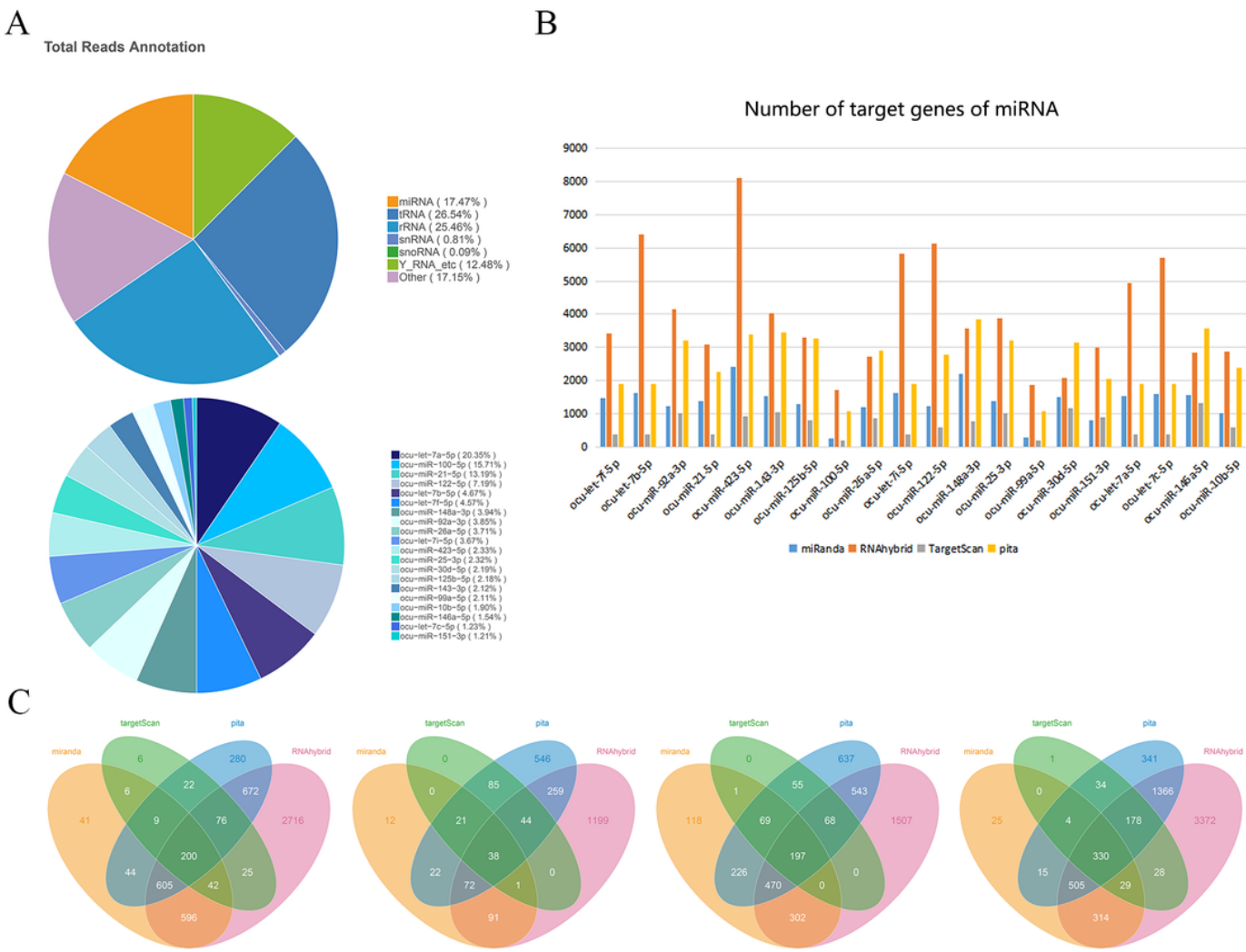

Figure 4

High-throughput sequencing and analysis of OB-exos. (A) Distribution of the internal components of exosomes and the percentage of the top 20 miRNAs among the total miRNAs in the exosomes. (B) The number of target genes the top 20 miRNAs were determined with four software programs. (C) The intersections of the target genes of the top four most abundant miRNAs determined with four software programs are displayed in a Venn diagram. From left to right: let-7a-5p, miR-100-5p, miR-21-5p and miR-122-5p.

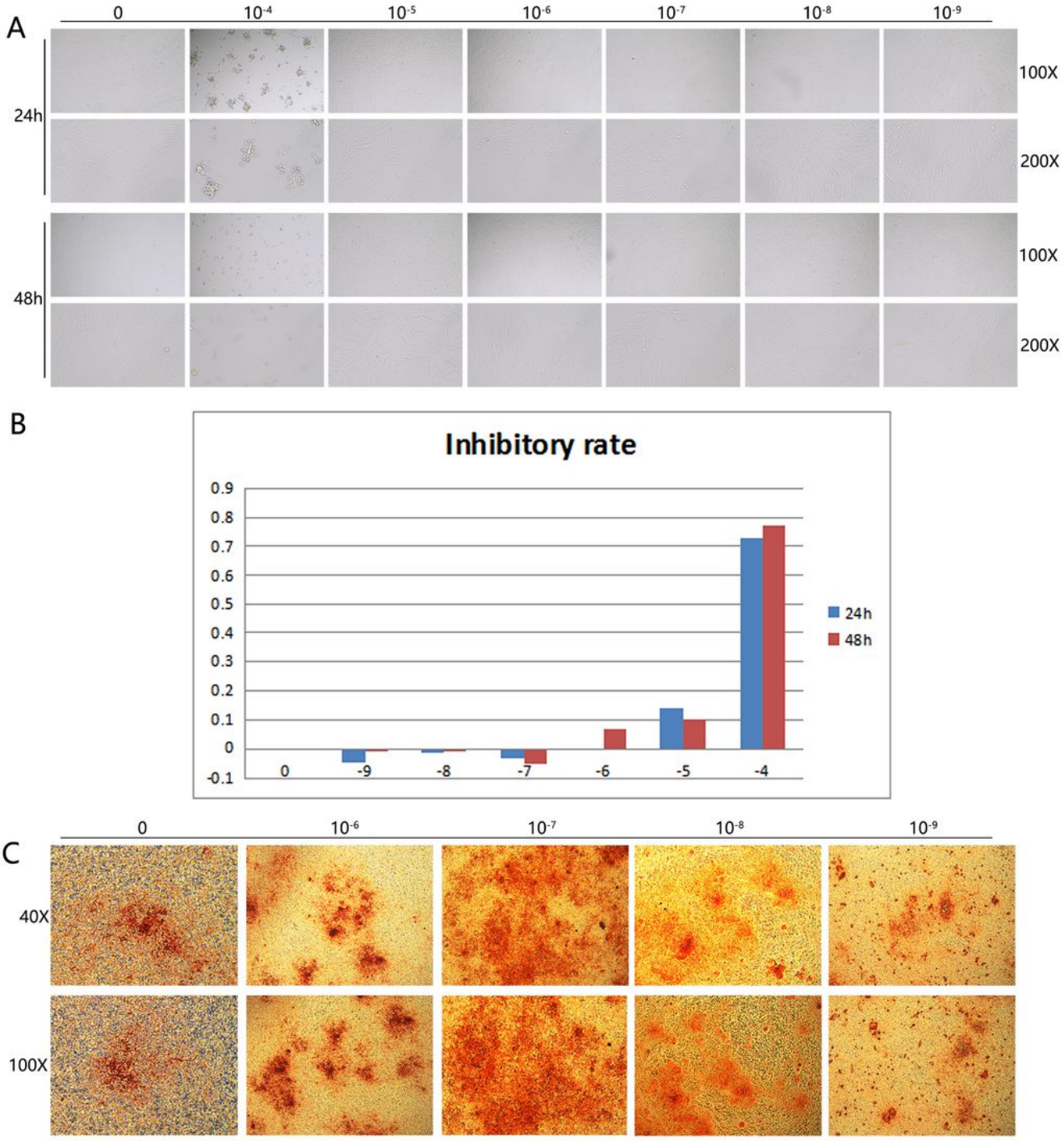

Figure 5

Detection of the activity, proliferation and of mineralization BMSCs under the action of ICA. (A) BMSCs treated with different concentrations of ICA were observed by microscopy under different magnifications. (B) A CCK-8 assay kit was used to detect the effects of ICA at various concentrations on BMSCs at 24 h and 48 h. The inhibitory effects on activity and proliferation are shown. (C) After 2 weeks of culture and

staining with Alizarin Red, the mineralized nodules of BMSCs cultured with different concentrations of ICA were observed by microscopy.

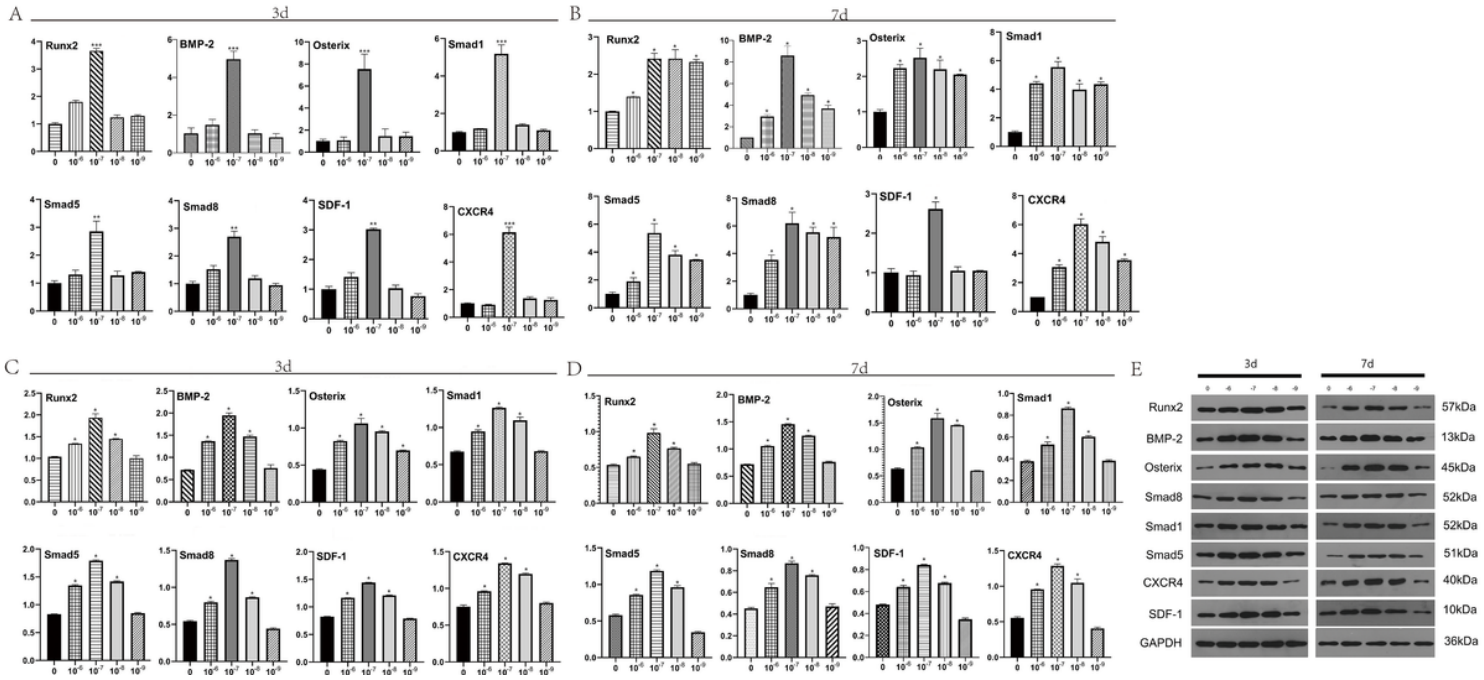

Figure 6

The effects of different concentrations of ICA on the osteogenic differentiation and migration of BMSCs. (A) and (B) show the mRNA expression of genes related to osteogenic differentiation and migration was detected by qPCR. (C-E) show the protein expression of genes related to osteogenic differentiation and migration was detected by Western blot.

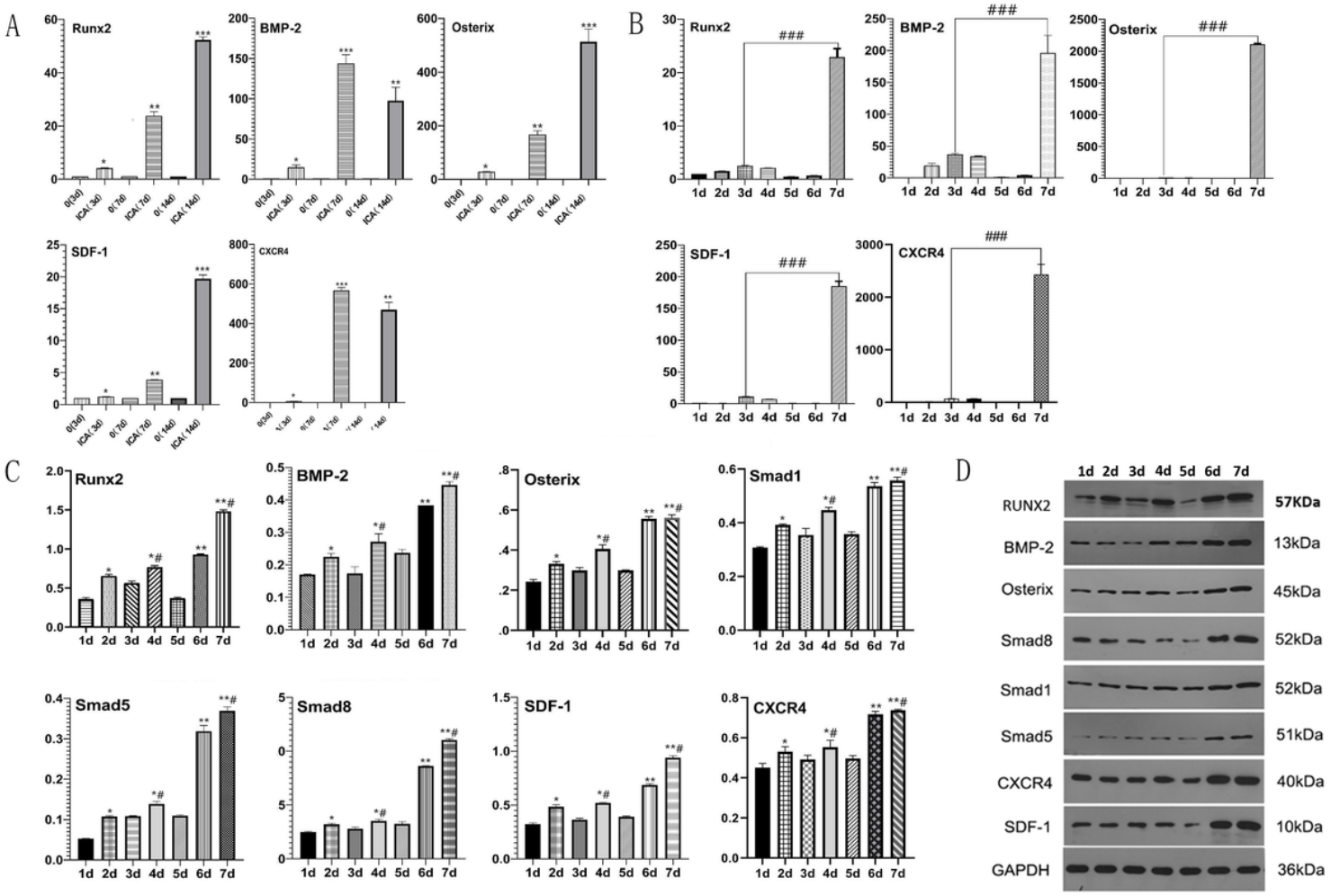

Figure 7

Effects of ICA on the osteogenic differentiation and migration of BMSCs during different stages. (A) The mRNA expression of osteogenic-related genes and migration-related genes on the 3rd day, 7th day, and 14th day. (B) ICA at a concentration of 1×10^{-7} M affected the mRNA expression of osteogenic-related genes and migration-related genes from days 1-7. (C) and (D) ICA at a concentration of 1×10^{-7} M affected the proteins expression of osteogenic-related and migration-related genes from days 1-7. * or # $p<0.05$, ** or ## $p<0.01$, *** or ### $p<0.001$;

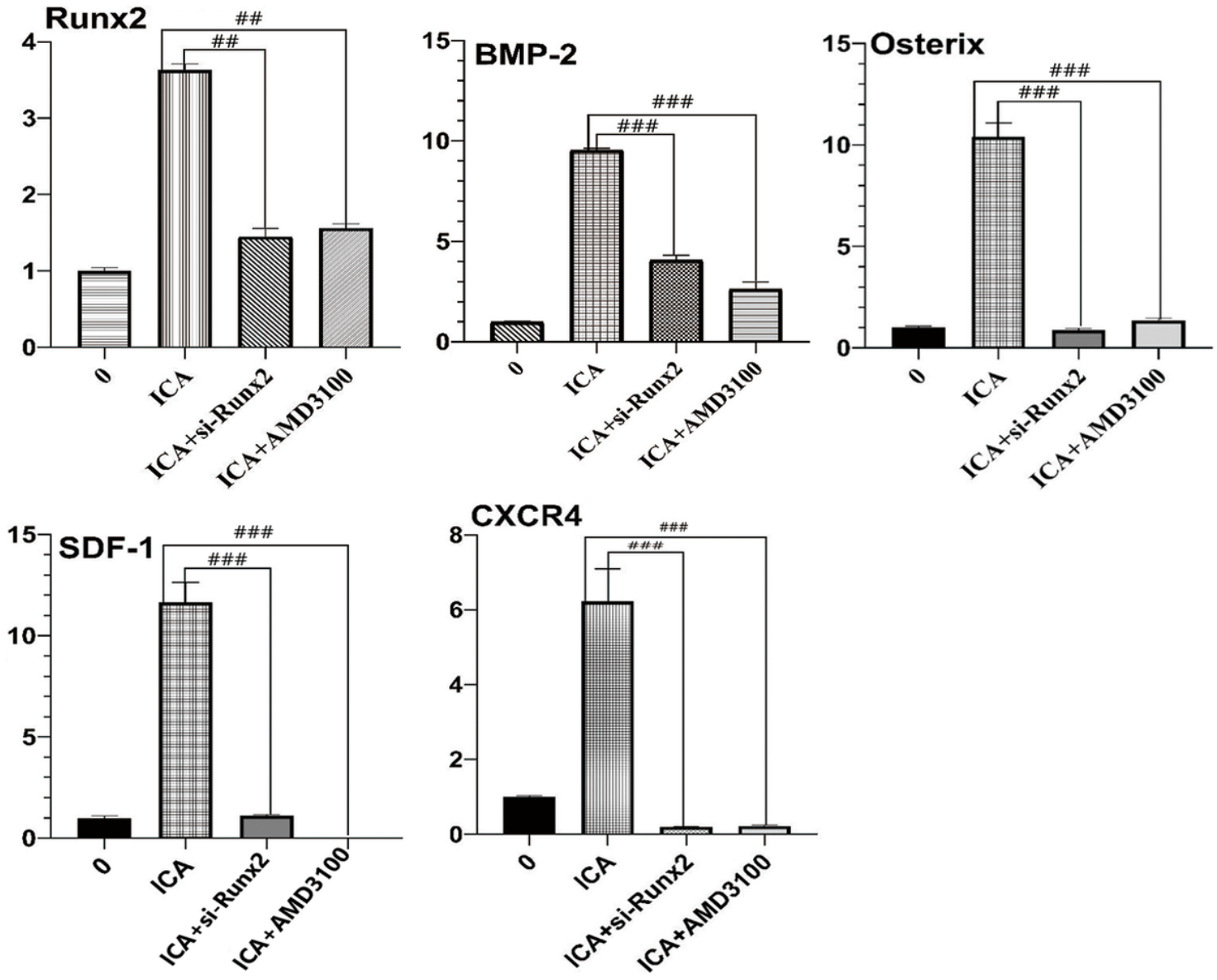

Figure 8

The role of ICA on osteogenic differentiation and migration through signalling pathway detection. BMSCs were treated with 0 M ICA, 1×10^{-7} M ICA, 1×10^{-7} M ICA +si-Runx2 and 1×10^{-7} M ICA +AMD3100. ## $p<0.01$, ### $p<0.001$.

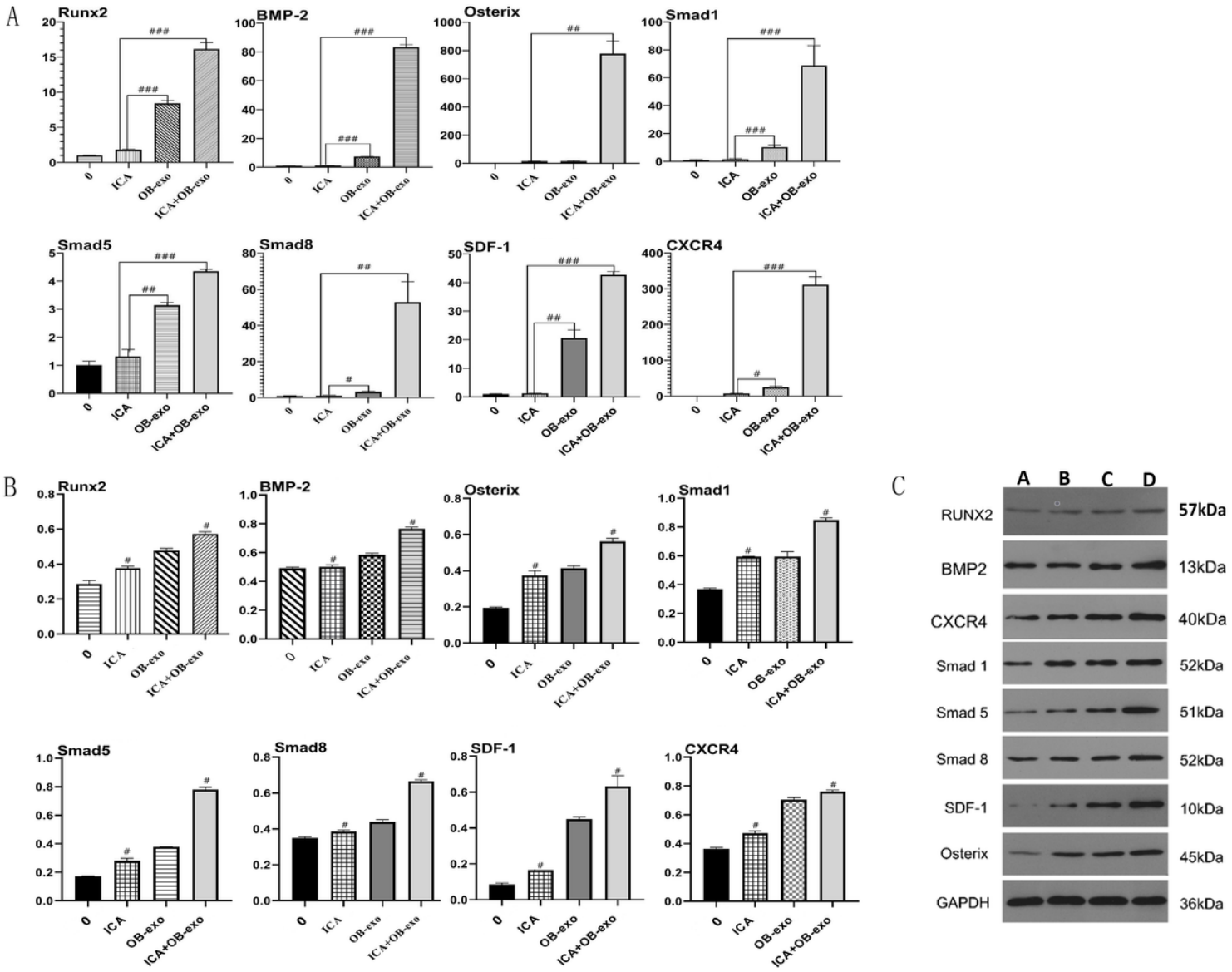

Figure 9

ICA combined with OB-exos affected the osteogenic differentiation and migration of BMSCs. (A) The mRNA expression of osteogenesis-related and migration-related genes was examined by qPCR. (B-C) The protein expression of osteogenesis-related and migration-related genes was examined by Western blot. # $p<0.05$, #$^{\#}$ $p<0.01$, #$^{\#\#}$ $p<0.001$.

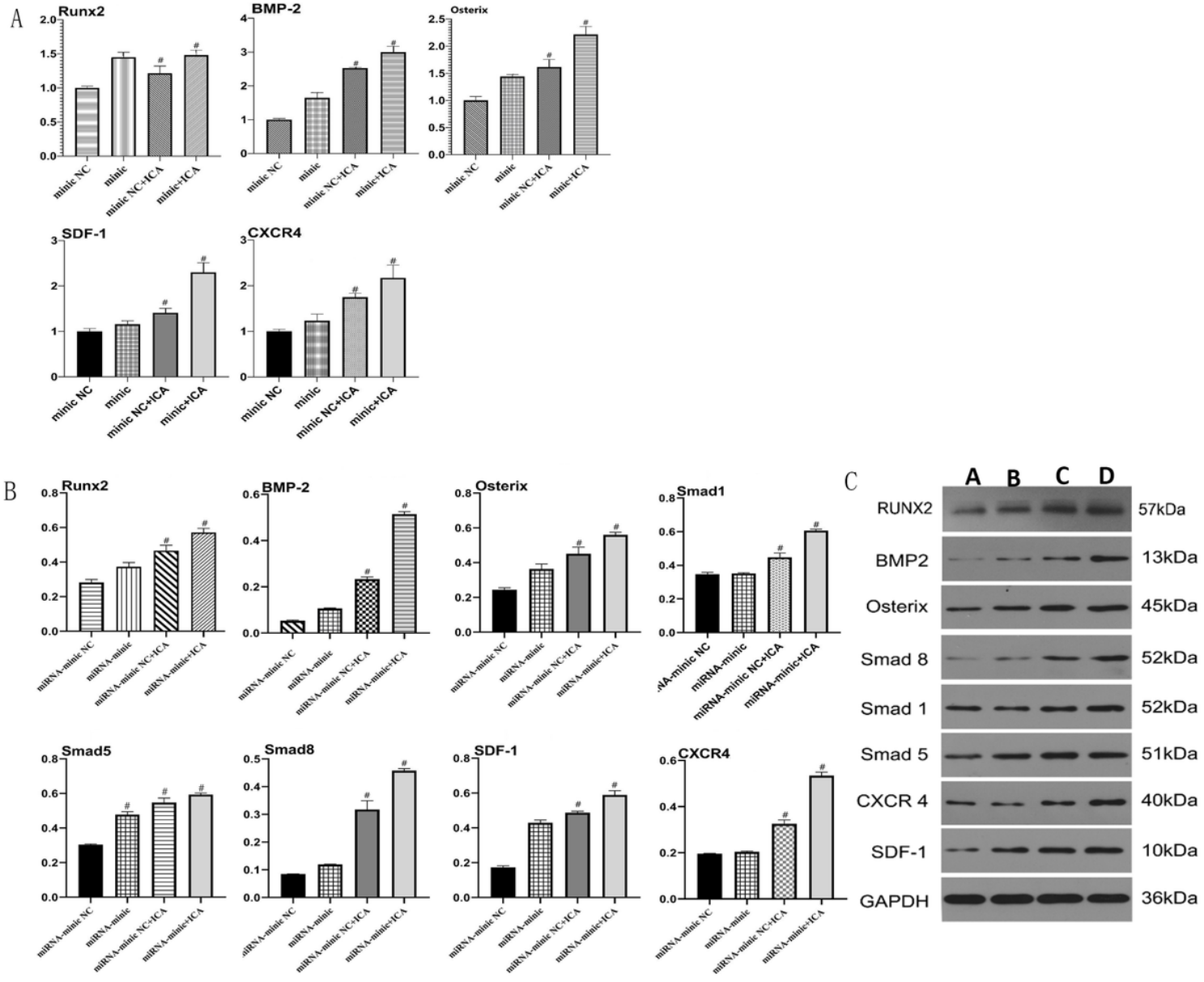

Figure 10

Detection the effects of combing treatment with ICA and miR-122-5p mimic on the osteogenic differentiation and migration of BMSCs. (A) The mRNA expression of osteogenic differentiation-related and migration-related genes in the miR-122-5p mimic NC group, miR-122-5p mimic group, miR-122-5p-mimic NC+ICA group, and miR-122-5p mimic +ICA group. (B-C) The proteins expression of osteogenic differentiation-related and migration-related genes. # $p<0.05$.

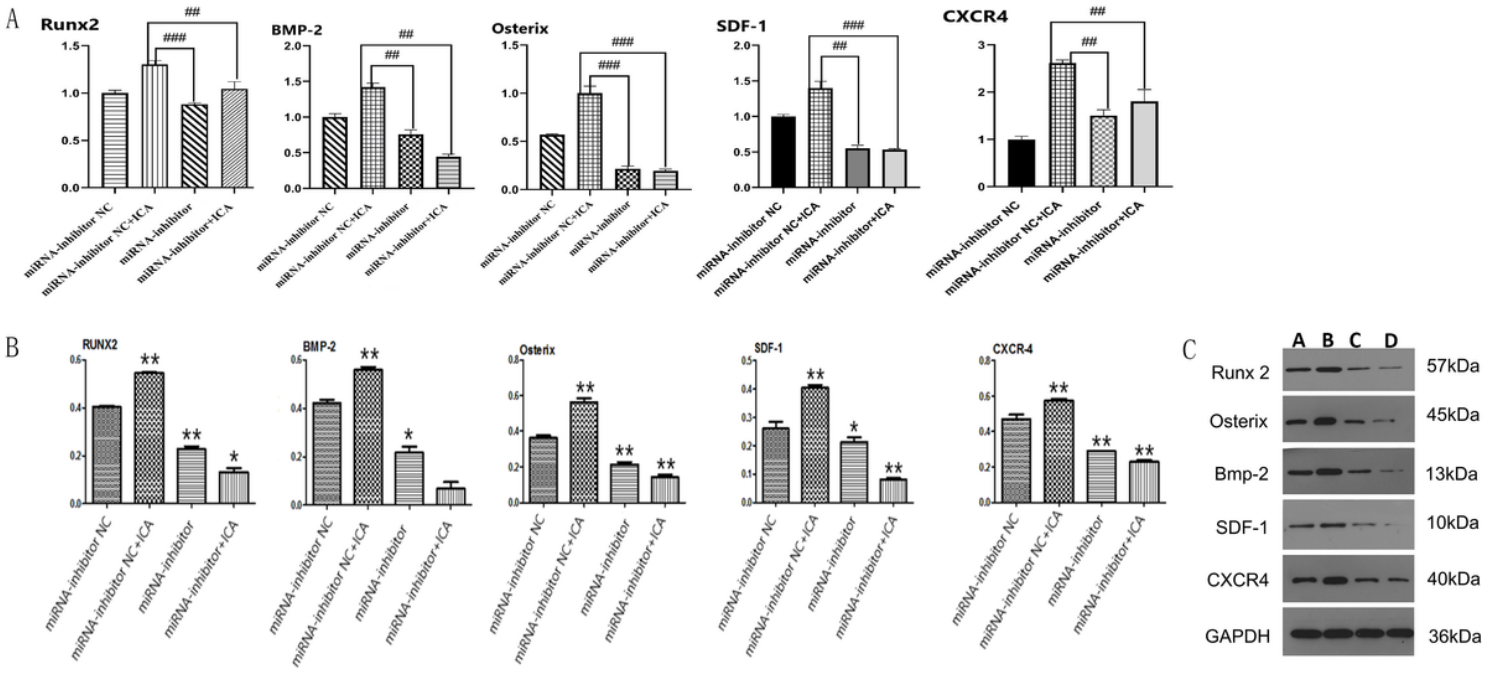

Figure 11

Investigation of the effects of combination treatment with ICA and miR-122-5p inhibitor on the osteogenic differentiation and migration of BMSCs. (A) The mRNA expression of genes related to osteogenic differentiation and migration in the miR-122-5p inhibitor NC group, miR-122-5p inhibitor NC+ICA group, miR-122-5p inhibitor group, and miR-122-5p inhibitor +ICA group. ## p<0.01, ### p<0.001. (B-C) The proteins expression of osteogenic differentiation-related and migration-related genes. * p<0.05, ** p<0.01.